LETTER

https://doi.org/10.1038/s41586-018-0676-z

Urbanization exacerbated the rainfall and flooding caused by hurricane Harvey in Houston

Wei Zhang[1], Gabriele Villarini[1]*, Gabriel A. Vecchi[2,3] & James A. Smith[4]

Category 4 landfalling hurricane Harvey poured more than a metre of rainfall across the heavily populated Houston area, leading to unprecedented flooding and damage. Although studies have focused on the contribution of anthropogenic climate change to this extreme rainfall event[1–3], limited attention has been paid to the potential effects of urbanization on the hydrometeorology associated with hurricane Harvey. Here we find that urbanization exacerbated not only the flood response but also the storm total rainfall. Using the Weather Research and Forecast model—a numerical model for simulating weather and climate at regional scales—and statistical models, we quantify the contribution of urbanization to rainfall and flooding. Overall, we find that the probability of such extreme flood events across the studied basins increased on average by about 21 times in the period 25–30 August 2017 because of urbanization. The effect of urbanization on storm-induced extreme precipitation and flooding should be more explicitly included in global climate models, and this study highlights its importance when assessing the future risk of such extreme events in highly urbanized coastal areas.

North Atlantic tropical cyclones are among the costliest natural hazards both in terms of fatalities and economic impacts, with the devastation left by 2017 hurricanes Harvey, Irma and Maria typical of the havoc tropical cyclones can cause. There are multiple hazards associated with these events, including storm surge, strong winds, heavy rainfall and flooding. An analysis of 28 tropical cyclones over the 2001–2014 period found that around two-thirds of the residential flood insurance claims were caused by riverine flooding[4], highlighting the major impact of these events for both coastal and inland communities.

The devastation caused by hurricane Harvey in Houston is a reminder of the rainfall and flooding that can be associated with these storms. Between 25 and 30 August 2017, hurricane Harvey dropped more than 1,300 mm of rain over and around Houston, leading to unprecedented flooding in large areas of the city[1–3]. In the aftermath of this storm, different studies estimated the return period of the rainfall associated with this event and quantified the human-induced climate change signal using a combination of observations and climate models. In ref. [1] it was found that the return period of Harvey's rainfall was around 2,000 years in the late twentieth century, and predicted to drop to 100 years by the end of this century. In ref. [2] and ref. [3] it was found that human-induced climate change made this event between 1.5 and 5 times, or at least 3.5 times, more likely, respectively.

Thus, the literature on the anthropogenic contribution to hurricane Harvey has focused on precipitation and on the part that human-induced climate change may have played. Here, we seek to answer a complementary question related to the anthropogenic contribution to Harvey's flooding: to what extent did urbanization have a role in the heavy rainfall and flooding associated with hurricane Harvey? From a hydrologic perspective, increases in urbanization are expected to lead to faster runoff and larger peaks owing to the large reductions in infiltration (the amount of water the ground can absorb)[5,6]. Houston has had the largest urban growth and the fifth-largest population growth in the United States over the period 2001–2011[7]. The increase in asphalt and concrete has led to an increasing runoff ratio (that is, the ratio between runoff and precipitation) across many watersheds in the area, pointing to reduced infiltration and larger runoff for a given rainfall value[8–12]. This increase in population and urbanization, combined with the flat clay terrain that characterizes this area, represents a very problematic mix from a flood perspective, despite the flood mitigation measures that have been put in place.

In addition to having a substantial impact on the hydrologic response, urbanization has the potential to directly influence the magnitude of extreme precipitation. This is a topic that has received substantial attention, particularly regarding the influence of urbanization on mesoscale convective systems, as determined through field campaigns, analysis

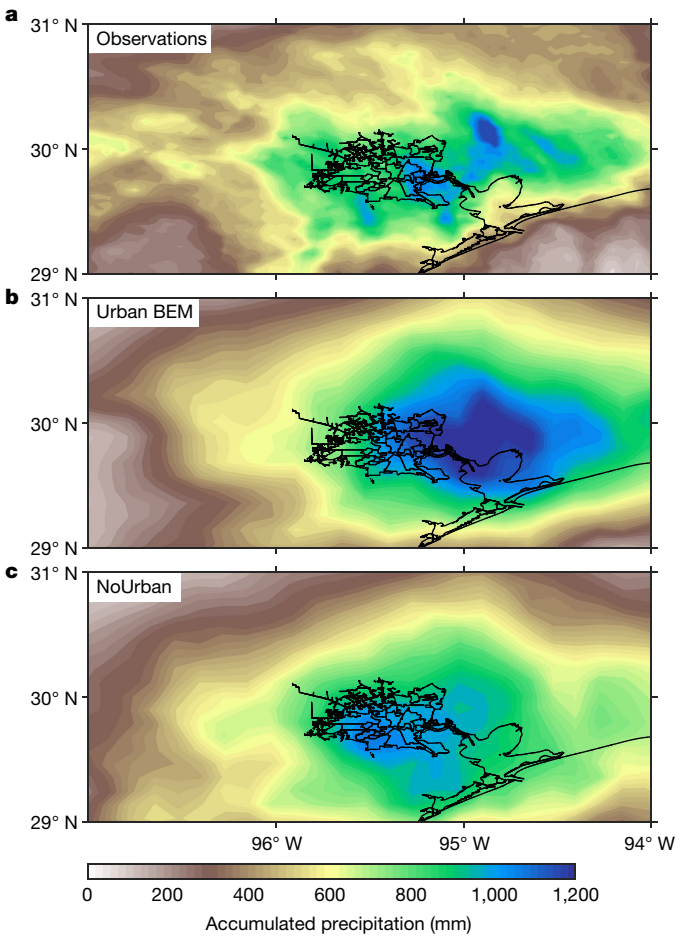

Fig. 1 | Storm total rainfall by hurricane Harvey. a–c, Accumulated precipitation for 25–30 August 2017 in observations (**a**), and in the 'Urban BEM' (**b**) and 'NoUrban' (urban land-use types replaced by croplands; **c**) WRF experiments. The model results represent the average of the seven members.

[1]IIHR-Hydroscience & Engineering, The University of Iowa, Iowa City, IA, USA. [2]Department of Geosciences, Princeton University, Princeton, NJ, USA. [3]Princeton Environmental Institute, Princeton University, Princeton, NJ, USA. [4]Department of Civil and Environmental Engineering, Princeton University, Princeton, NJ, USA. *e-mail: gabriele-villarini@uiowa.edu

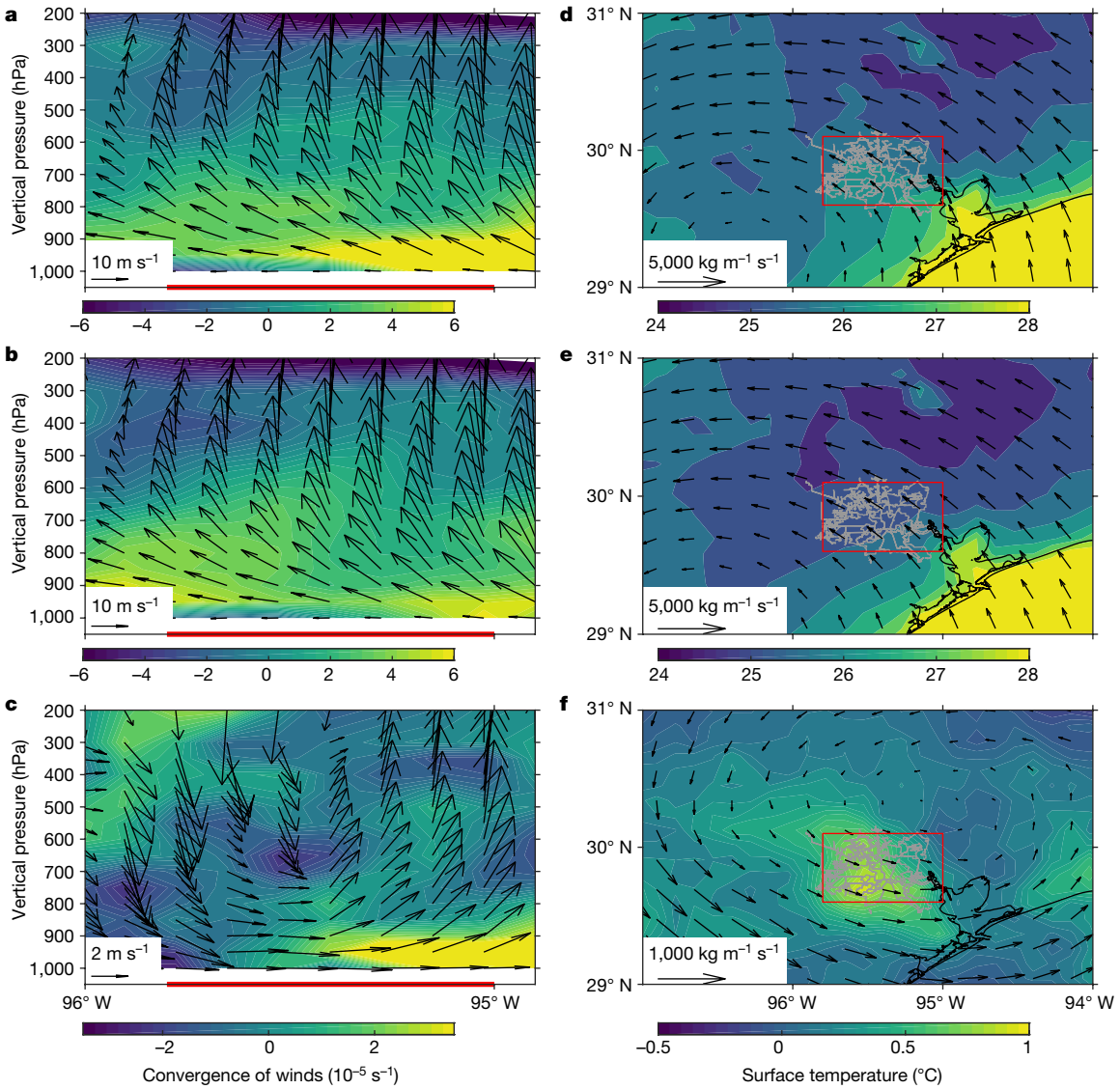

Fig. 2 | Key variables for diagnosing the effects of urbanization on hurricane Harvey. a–c, The vertical profile of wind convergence (colour scale) and zonal and vertical wind speed and direction (vertical wind speed shown here has been multiplied by 100, indicated by arrows) averaged over Houston (red rectangles in **d–f**) for 25–30 August 2017 for the 'Urban BEM' (**a**) and 'NoUrban' (**b**) experiments and their differences (**c**). The red lines at the bottom represent the zonal extent of Houston. **d–f**, The daily averaged vertically integrated moisture flux (indicated by arrows) and surface temperature (colour scale) for 25–30 August 2017 for the 'Urban BEM' (**d**) and 'NoUrban' (**e**) experiments with WRF and their differences (**f**).

of observations and numerical modelling. Much of the research on the topic has, however, focused on convective systems and how the urban area affects the trajectory of the convective cells[13–15]. Much less is known regarding the urban effects on the organized tropical rainfall of a hurricane, in particular during one like hurricane Harvey, which stalled for several days. Overall, the role of the city in altering both the rainfall and runoff responses has received very limited attention, especially in the context of tropical cyclones.

Because of the substantial hydrometeorological impacts of urbanization, here we want to quantify the part that urban development of Houston has played during hurricane Harvey by accounting for both changes in total rainfall and flood response. We start by examining the role of urbanization in terms of storm total rainfall; these analyses are then followed by a focus on the hydrologic response, and we conclude our study by quantifying the impact of Houston on the flooding from hurricane Harvey. Combined with the assessments of the climate-mediated anthropogenic impacts on hurricane Harvey[1–3], this work will enable a fuller assessment of the total anthropogenic contribution to the flooding from this storm.

To explore urban and hydrometeorological impacts on rainfall during hurricane Harvey, we performed two sets of seven-member experiments with the WRF model (see Methods). In the first set ('Urban BEM'), we simulate hurricane Harvey by using WRF coupled with the Noah land surface model and the multi-layer building energy model (BEM). The second set of experiments ('NoUrban') is performed with the same setting as the first one, but with croplands replacing urban land-use types. The differences in rainfall between the two experiments represent the impacts of urbanization on Harvey's total rainfall. During 25–30 August 2017, hurricane Harvey was responsible for more than 1,000 mm of rainfall over the Houston area, in particular over the southeastern part of the city (Fig. 1a). Overall, the 'Urban BEM' experiments capture reasonably well many aspects of the observed rainfall during this period (Fig. 1b). From a quantitative perspective, the rainfall totals during Harvey in the 'Urban BEM' experiments are comparable with those observed (Fig. 1a, b). In contrast, the 'NoUrban' experiments produce much less precipitation than the 'Urban BEM' ones, with the rainfall maxima shifted west with respect to the 'Urban BEM' runs. The differences in accumulated rainfall between 'Urban

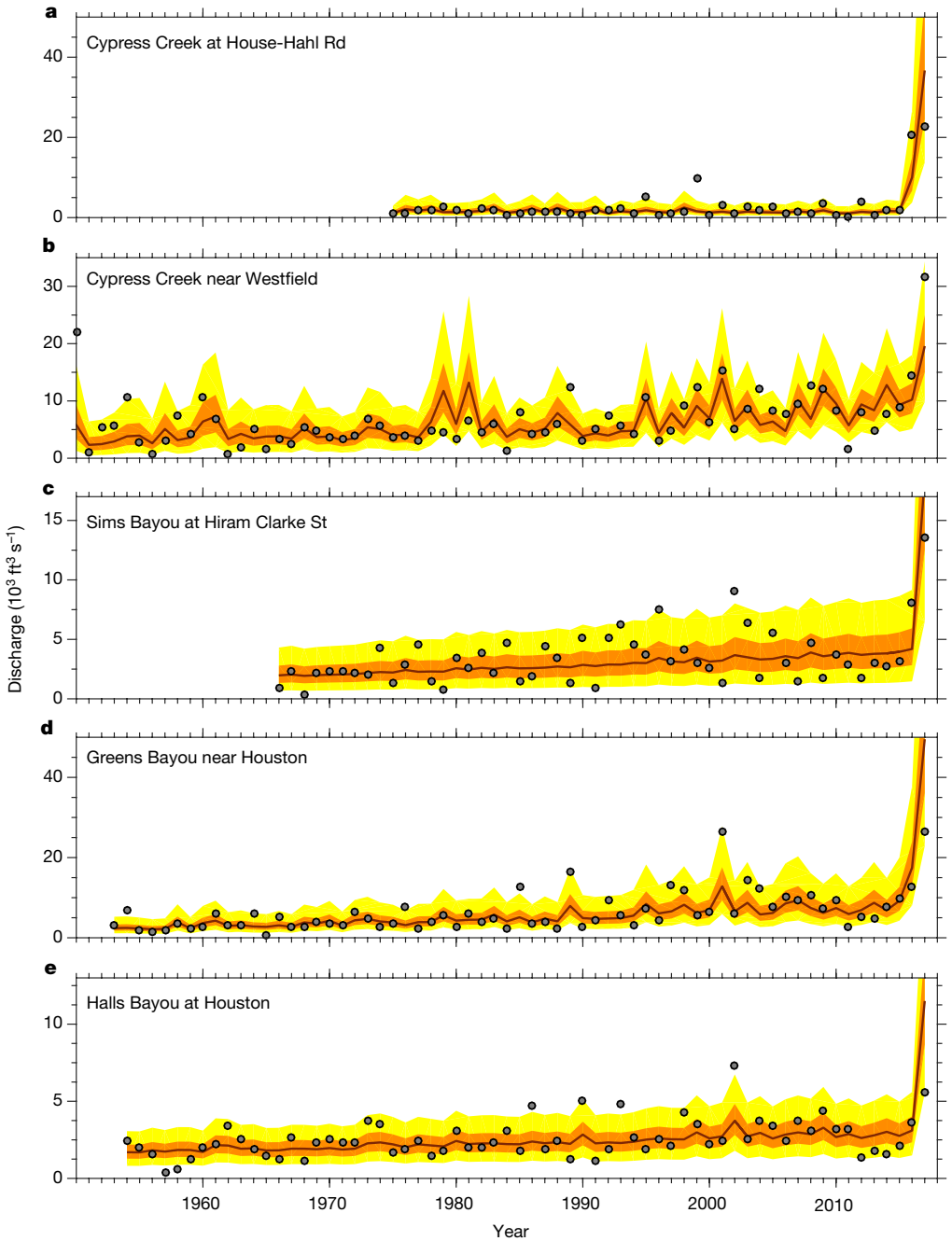

Fig. 3 | Modelling of the annual maximum peak discharge records. **a**–**e**, Modelling of the annual maximum peak discharge records at the five sites considered here (see Extended Data Fig. 5 and Extended Data Table 1a for more information). The circles are the observations; the dark red solid lines represent the median of the fitted distribution, while the yellow (orange) areas indicate the 5th to 95th (25th to 75th) percentiles.

BEM' and 'NoUrban' experiments clearly show a large increase in rainfall arising from urbanization over the eastern part of the Houston area (Extended Data Fig. 1). Moreover, the western shift in rainfall maxima in 'NoUrban' experiments leads to more rainfall in the western part of Houston than that in the 'Urban BEM' case (Extended Data Fig. 1). These statements are also supported by statistical analyses, which indicate that these differences are statistically significant at the $P < 0.05$ level (Extended Data Fig. 1). Urbanization led to an amplification of the total rainfall along with a shift in the location of the maximum rainfall.

The enhanced rainfall in the 'Urban BEM' case and the shift of rainfall in the 'NoUrban' case are tied to the storm system's drag induced by large surface roughness. Extended Data Fig. 2 shows accumulated rainfall during 25–30 August 2017 in each member of the 'Urban BEM' and 'NoUrban' experiments. Overall, the rainfall maximum in the 'Urban BEM' experiments shifts eastward compared with the corresponding 'NoUrban' experiments for each ensemble member (Extended Data Fig. 2), similar to the ensemble mean of the results (Fig. 1) associated with the drag effects by the urban surface roughness (Extended Data Fig. 3). The consistency in the results among ensemble members lends confidence to the robustness of the impacts of urbanization in total rainfall associated with hurricane Harvey.

To further understand the physical mechanisms responsible for the enhanced rainfall due to urbanization, we analyse the vertical profile of convergence of winds and wind fields, and the 2-m surface temperature in the WRF experiments. Figure 2 shows an enhancement of the low-level convergence and of the divergence above 600 hPa in the 'Urban BEM' experiment compared to the 'NoUrban' one. The difference between these two experiments indicates enhanced low-level convergence, upper-level divergence and anomalous ascent over Houston, leading to favourable conditions for precipitation (Fig. 2c).

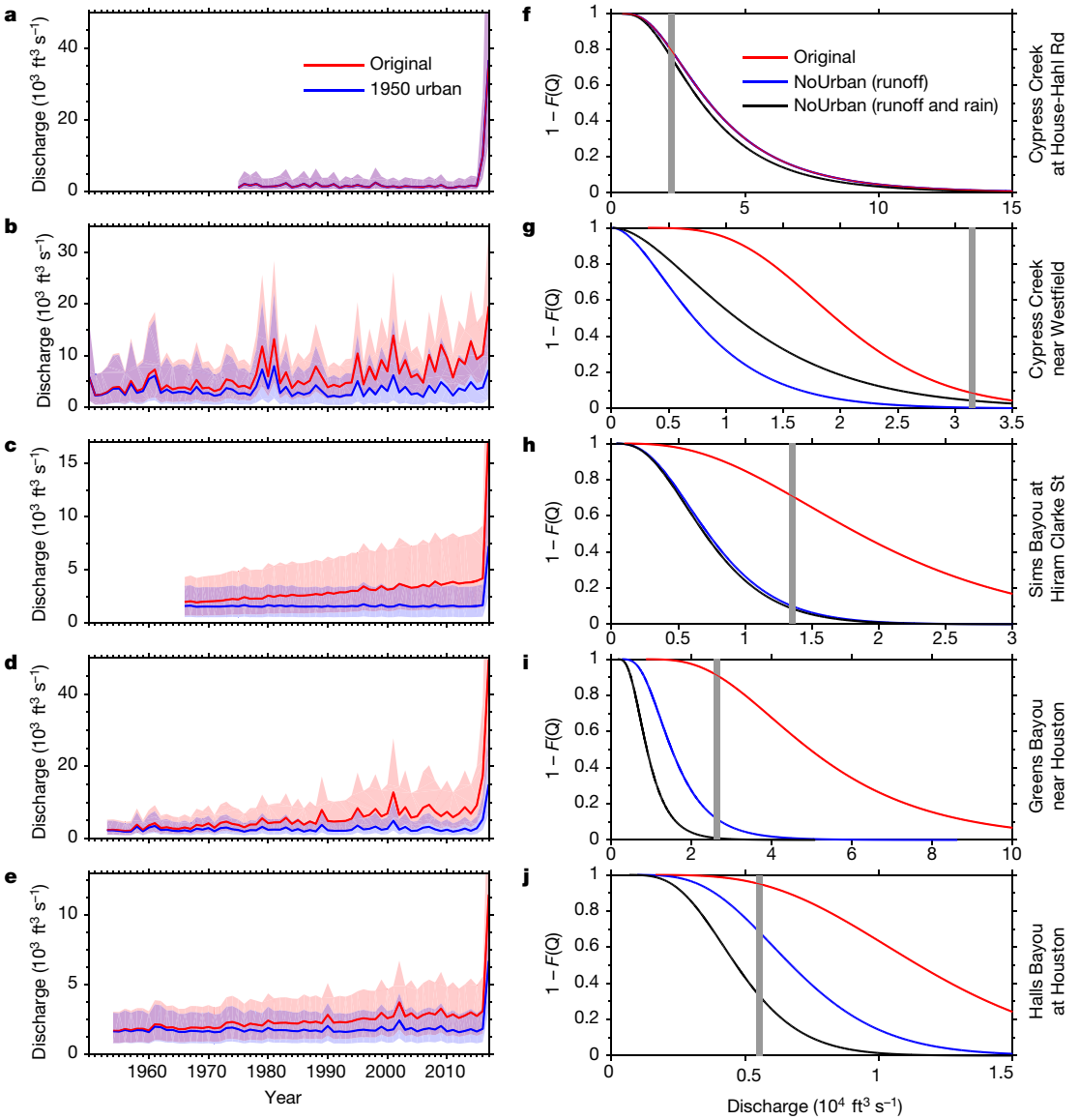

Fig. 4 | Examination of the effects of urbanization on the modelled annual maximum discharge. a–e, Modelled annual maximum discharge Q with original urbanization represented by population (red) and that in 1950 ('1950 urban', blue) for the five sites considered here. The shading represents the values within the 5th–95th percentile of the modelled annual maximum discharge. **f–j**, The probability ($1 - F(Q)$) (where F is the fitted cumulative distribution function of Q) of having the value of annual maximum discharge with respect to urbanization as observed (red), with urbanization kept at the 1950 level (blue), and with urbanization kept at the 1950 level and rainfall scaled by the related change between 'Urban BEM' and 'NoUrban' simulations for each basin (black). The grey bars represent the value of annual maximum discharge for 2017.

The difference between the 'Urban BEM' and 'NoUrban' simulations highlights the presence of a cyclonic flow pattern in the moisture flux, which is also favourable for precipitation (Fig. 2d–f). Such differences in convergence and updraft are probably caused by the drag of urban surface with large roughness, associated with stronger friction velocity and roughness length in the 'Urban BEM' experiments (Extended Data Fig. 3a–f). Specifically, the friction velocity in the 'Urban BEM' simulation is markedly larger than the 'NoUrban' simulation (Extended Data Fig. 3a–c), indicating a stronger drag on the storm winds, associated with a larger surface roughness length (Extended Data Fig. 3d–f). The changes in sensible heat flux and Bowen ratio (Extended Data Fig. 3g–i) associated with urbanization and urban land-use change may lead to the destabilization of the atmosphere[16–20], enhancing rainfall over the eastern side of Houston. The increased urban roughness and surface warming are also associated with elevated height of the bottom boundary layer of the atmosphere, which tends to enhance precipitation (Extended Data Fig. 3j–l). These results point to the combined effects of surface drag and urban surface warming on rainfall enhancement on the eastern side of Houston. Moreover, anthropogenic heat may influence precipitation in urban areas[21]. The 'Urban BEM' experiments can explicitly resolve anthropogenic heat to a large extent by computing anthropogenic heat using a parameterization scheme[21,22]. Overall, rainfall over Houston in the 'Urban BEM' experiment is consistent with the results from the 'Urban BULK' experiments in which no urban canopy model is coupled with the Noah land surface model (Extended Data Fig. 4), suggesting that anthropogenic heat does not play a major part in rainfall related to hurricane Harvey.

Thus we have focused on the impacts of Houston on precipitation and provided a physical understanding of these results. However, urbanization also affects hydrologic processes, so we next quantify the role of urbanization following an approach used in ref. [23] (see Methods). Our modelling results suggest that the year-to-year variations in annual maximum peak discharge are well captured by parsimonious statistical models relating the maximum peak discharge to precipitation and/or population (used as proxy for urbanization, see Methods) (Fig. 3). This is also supported by the goodness-of-fit diagnostics (Extended

Data Fig. 6 and Extended Data Table 2). On the basis of our modelling results, urbanization is an important predictor in controlling the magnitude and variability in the flood peak record at all the sites, with the exception of Cypress Creek at House-Hahl Road near Cypress (USGS ID 08068740), which is also the basin that can be considered as the control watershed area owing to the very limited amount of urbanization it has experienced (Extended Data Fig. 5).

To quantify the role of urbanization in terms of flooding, we use these statistical models with the observed rainfall but with urbanization kept constant at the 1950 level (that is, representative of the pre-urbanization conditions) (Fig. 4a–e). For Cypress Creek at House-Hahl Road near Cypress the results are the same, given that urbanization is not an important predictor. For the other four watersheds, there is a clear increase in the magnitude and variability associated with the urban expansion of Houston. To assess the role of hurricane Harvey, we focus on 2017 and quantify the effect of urbanization in terms of both flooding and rainfall. Figure 4f–j shows the probability of exceedance for the fitted distribution with the parameters that depend on the values of the predictors in 2017. It also shows the same results but using: (1) the value of urbanization in 1950 but the observed precipitation; and (2) the value of urbanization in 1950 and storm total rainfall scaled by the related change between 'Urban BEM' and 'NoUrban' simulations for each basin. From these results, we conclude that urbanization played an important part during this event, as shown by the shift to the left in the survival function, with changes in both hydrologic response and precipitation strongly affecting these watersheds. We also computed the risk ratio[24] (see Methods), which indicates that, on average, urbanization has increased the probability of an event like the flooding associated with hurricane Harvey by about 21 times (Extended Data Table 1a). Therefore, urbanization strongly exacerbated the impact that this storm has had in terms of both precipitation and flood response.

Given that hurricane winds and rainfall are projected to intensify in the future[25,26] and urbanization is also expected to continue increasing in the major coastal cities, our work paves the way towards increasing our understanding of the risk arising from the interconnection between anthropogenic effects from urbanization and those mediated through climatic influences on hurricane-related rainfall. Planning must take into account the compounded nature of these risks, and efforts to build flood mitigation strategies must use an improved understanding of the multiple processes in place[27]. Failure to account for urban factors would jeopardize the investment in mitigation and management of climate change impacts[28]. Given the small scales at which an event of this kind operates in terms of urban impacts and responses, it is critical for the next generations of global climate models to be able to resolve the urban areas and their associated processes through increasing spatial resolution and improved representation of the processes that occur within the cities[29,30].

Online content

Any methods, additional references, Nature Research reporting summaries, source data, statements of data availability and associated accession codes are available at https://doi.org/10.1038/s41586-018-0676-z.

Received: 16 April 2018; Accepted: 7 September 2018;
Published online 14 November 2018.

1. Emanuel, K. Assessing the present and future probability of hurricane Harvey's rainfall. *Proc. Natl Acad. Sci. USA* **114**, 12681–12684 (2017).
2. Jan van Oldenborgh, G. et al. Attribution of extreme rainfall from Hurricane Harvey, August 2017. *Environ. Res. Lett.* **12**, 124009 (2017).
3. Risser, M. D. & Wehner, M. F. Attributable human-induced changes in the likelihood and magnitude of the observed extreme precipitation during hurricane Harvey. *Geophys. Res. Lett.* **44**, 12457–12464 (2018).
4. Czajkowski, J., Villarini, G., Montgomery, M., Michel-Kerjan, E. & Goska, R. Assessing current and future freshwater flood risk from North Atlantic tropical cyclones via insurance claims. *Sci. Rep.* **7**, 41609 (2017).
5. Smith, J. A. et al. The regional hydrology of extreme floods in an urbanizing drainage basin. *J. Hydrometeorol.* **3**, 267–282 (2002).
6. Smith, J. A. et al. Extraordinary flood response of a small urban watershed to short-duration convective rainfall. *J. Hydrometeorol.* **6**, 599–617 (2005).
7. Bounoua, L., Nigro, J., Zhang, P., Thome, K. & Lachir, A. Mapping urbanization in the United States from 2001 to 2011. *Appl. Geogr.* **90**, 123–133 (2018).
8. Johnson, S. L. & Sayre, D. M. *Effects of Urbanization on Floods in the Houston, Texas Metropolitan Area*. Report No. 73-3, https://pubs.er.usgs.gov/publication/wri733 (US Geological Survey, 1973).
9. Liscum, F. *Effects of Urban Development on Stormwater Runoff Characteristics for the Houston, Texas, Metropolitan Area.* Report No. 2001-4071, https://pubs.er.usgs.gov/publication/wri014071 (US Geological Survey, 2001).
10. Khan, S. D. Urban development and flooding in Houston Texas, inferences from remote sensing data using neural network technique. *Environ. Geol.* **47**, 1120–1127 (2005).
11. Zhu, L., Quiring, S. M., Guneralp, I. & Peacock, W. G. Variations in tropical cyclone-related discharge in four watersheds near Houston, Texas. *Clim. Risk Manage.* **7**, 1–10 (2015).
12. Muñoz, L. A., Olivera, F., Giglio, M. & Berke, P. The impact of urbanization on the streamflows and the 100-year floodplain extent of the Sims Bayou in Houston, Texas. *Int. J. River Basin Manage.* **16**, 61–69 (2018).
13. Ntelekos, A. A. et al. Extreme hydrometeorological events and the urban environment: dissecting the 7 July 2004 thunderstorm over the Baltimore MD metropolitan region. *Wat. Resour. Res.* **44**, W08446 (2008).
14. Niyogi, D., Lei, M., Kishtawal, C., Schmid, P. & Shepherd, M. Urbanization impacts on the summer heavy rainfall climatology over the eastern United States. *Earth Interact.* **21**, 1–17 (2017).
15. Niyogi, D. et al. Urban modification of thunderstorms: an observational storm climatology and model case study for the Indianapolis urban region. *J. Appl. Meteorol. Climatol.* **50**, 1129–1144 (2011).
16. Oke, T. R. The energetic basis of the urban heat island. *Q. J. R. Meteorol. Soc.* **108**, 1–24 (1982).
17. Shepherd, J. M., Carter, M., Manyin, M., Messen, D. & Burian, S. The impact of urbanization on current and future coastal precipitation: a case study for Houston. *Environ. Plann. B* **37**, 284–304 (2010).
18. Baik, J.-J., Kim, Y.-H. & Chun, H.-Y. Dry and moist convection forced by an urban heat island. *J. Appl. Meteorol.* **40**, 1462–1475 (2001).
19. Voogt, J. A. & Oke, T. R. Thermal remote sensing of urban climates. *Remote Sens. Environ.* **86**, 370–384 (2003).
20. Shepherd, J. M. A review of current investigations of urban-induced rainfall and recommendations for the future. *Earth Interact.* **9**, 1–27 (2005).
21. Sharma, A. et al. Urban meteorological modeling using WRF: a sensitivity study. *Int. J. Climatol.* **37**, 1885–1900 (2017).
22. Salamanca, F., Martilli, A., Tewari, M. & Chen, F. A study of the urban boundary layer using different urban parameterizations and high-resolution urban canopy parameters with WRF. *J. Appl. Meteorol. Climatol.* **50**, 1107–1128 (2011).
23. Villarini, G. et al. Flood frequency analysis for nonstationary annual peak records in an urban drainage basin. *Adv. Water Resour.* **32**, 1255–1266 (2009).
24. Paciorek, C. J., Stone, D. A. & Wehner, M. F. Quantifying uncertainty in the attribution of human influence on severe weather. Preprint at https://arxiv.org/abs/1706.03388 (2017).
25. Knutson, T. R. et al. Tropical cyclones and climate change. *Nat. Geosci.* **3**, 157–163 (2010).
26. Sobel, A. H. et al. Human influence on tropical cyclone intensity. *Science* **353**, 242–246 (2016).
27. Fang, Z., Dolan, G., Sebastian, A. & Bedient, P. B. Case study of flood mitigation and hazard management at the Texas Medical Center in the wake of tropical storm Allison in 2001. *Nat. Hazards Rev.* **15**, 05014001 (2014).
28. Pielke, R. A. et al. Land use/land cover changes and climate: modeling analysis and observational evidence. *WIREs Clim. Chang.* **2**, 828–850 (2011).
29. Lawrence, D. M. et al. The CCSM4 land simulation, 1850–2005: assessment of surface climate and new capabilities. *J. Clim.* **25**, 2240–2260 (2012).
30. Li, D., Malyshev, S. & Shevliakova, E. Exploring historical and future urban climate in the Earth System Modeling framework: 2. Impact of urban land use over the continental United States. *J. Adv. Model. Earth Syst.* **8**, 936–953 (2016).

Acknowledgements This material is based in part on work supported by the National Science Foundation under CAREER grant AGS-1349827 (to G.V.), NSF grant EAR-1520683 (to J.A.S. and G.A.V.), NSF grant AGS-1522492 and grant CBET-1444758 (to J.A.S.), and award NA14OAR4830101 from the National Oceanic and Atmospheric Administration, US Department of Commerce. G.A.V. was supported in part by The Carbon Mitigation Initiative at Princeton University.

Reviewer information *Nature* thanks A. Sharma and the other anonymous reviewer(s) for their contribution to the peer review of this work.

Author contributions W.Z. and G.V. designed the experiments and performed the analyses. All authors interpreted the results and wrote the paper.

Competing interests The authors declare no competing interests.

Additional information
Extended data is available for this paper at https://doi.org/10.1038/s41586-018-0676-z.
Supplementary information is available for this paper at https://doi.org/10.1038/s41586-018-0676-z.
Reprints and permissions information is available at http://www.nature.com/reprints.
Correspondence and requests for materials should be addressed to G.V.
Publisher's note: Springer Nature remains neutral with regard to jurisdictional claims in published maps and institutional affiliations.

METHODS

The observed rainfall data are obtained from the Stage IV Quantitative Precipitation Estimates products over the continental USA (CONUS, http://www.emc.ncep.noaa.gov/mmb/ylin/pcpanl/stage4/) released by the National Centers for Environmental Prediction (NCEP). The discharge data are obtained from the United States Geological Survey (USGS). The gauged daily precipitation data are downloaded from the Global Historical Climatology Network (ftp://ftp.ncdc.noaa.gov/pub/data/ghcn/daily/).

The numerical simulations for hurricane Harvey are performed with the Advanced Research WRF (ARW) core of the Weather Research and Forecasting (WRF) model version 3.8. The land-use data used for the WRF experiments are the National Land Cover Database 2011 (NLCD2011)[31] having 40 land-use categories including the types related to urban land-use: Developed Open Space (category 23), Developed Low Intensity (category 24), Developed Medium Intensity (category 25) and Developed High Intensity (category 26). In these four categories, the Developed Open Space category represents "areas with a mixture of some constructed materials, but mostly vegetation in the form of lawn grasses. Impervious surfaces account for less than 20% of total cover in this category"[32]. Because most of the surface of the Developed Open Space category is actually vegetation in the form of lawn grasses, we remapped only Developed Low Intensity (category 24), Developed Medium Intensity (category 25) and Developed High Intensity (category 26) into low-density residential, high-density residential and commercial use, respectively, by modifying the VEGPARM.TBL table under the WRF directory. We have plotted the remapped land-use map in the Houston area (Extended Data Fig. 7a). We run two sets of WRF experiments: one with the original land-use types by coupling Noah with the multi-layer building energy model ('Urban BEM')[33–35] and the other by replacing the urban land-use types with croplands ('NoUrban')[36]. The subtraction of precipitation in the multi-member 'NoUrban' from 'Urban BEM' experiments provides the impacts of urbanization on precipitation. 'Urban BEM' can be used to quantify the role of anthropogenic heat, given that previous studies have identified its influence on precipitation in urban areas[37–40]. The WRF experiments ('Urban BEM' and 'Urban BULK') in this study are designed for hurricane Harvey, which is a very strong and large system for which the improvements from the BEM model over the 'Urban BULK' model may be muted; however, this may not be the case for more localized convective rain events, for which the differences due to the urban schemes may be more important. The Noah land surface model is used and coupled with WRF ARW in the 'Urban BULK' experiments. The simulations with the BEM model allow us to account for the direct anthropogenic heat emission because anthropogenic heat is directly computed. We use three domains for the WRF simulations in this study with spatial resolution of 12 km, 4 km and 1.33 km, respectively (Extended Data Fig. 7b). The inside domain d03 covers Houston while the outer domain d01 covers the region 104° W to 87° W and 24° N to 25° N. Feedback is allowed from the nesting domains to their parent domains. To account for uncertainty, we have performed seven experiments for both the 'Urban BEM' and 'NoUrban' experiments by initializing WRF ARW on 23 August 0 h to 24 August 12 h 2017 at 6-h intervals. The initial and boundary conditions for the WRF runs are 3-h NCEP North American Regional Reanalysis products[41] (https://rda.ucar.edu/datasets/ds608.0/) on the Eta 221 grid at 29 pressure levels. The physics options are shown in Extended Data Table 1b.

The annual maximum flood peak data are based on the USGS measurements for the five watersheds shown in Extended Data Fig. 5 and Extended Data Table 1a (rather than using block maxima, an alternative approach would have been to use point processes, as has been advocated for in attribution studies[42]). At each site and for each of the annual maxima we computed the basin averaged rainfall by spatially interpolating the available daily rain gauges from the Global Historical Climatology Network. To identify the rainfall accumulation that is more closely correlated with the flood peaks, we computed the Spearman correlation between the flood peaks and the accumulated rainfall from the day of the event up to a week before it; the rainfall accumulation window with the largest Spearman correlation coefficient with respect to the annual maximum peak discharge was used for the analyses. We use population (divided by 10^{-4} so that its range of values is comparable to that for precipitation) as a proxy for urbanization[43–45], and interpolate the information from the US Census Bureau for the City of Houston from the decadal surveys (https://www.census.gov/prod/www/decennial.html) with a third-order polynomial function to obtain annual estimates, and assuming that all the watersheds have experienced the same urban growth. For the development of the statistical models, we considered two 2-parameter distributions (lognormal and gamma; see also refs [46–48]), and made their parameters linearly depend (via appropriate link functions) on every combination of the two predictors, with the only constraint that the location parameter included at least precipitation. Model selection is performed via the Schwarz Bayesian criterion as a compromise between accuracy and parsimony. We assess the goodness of fit of the models by means of visual examination of the worm plots[49] (Extended Data Fig. 6) and by computing the first four moments of the residuals and their Filliben correlation coefficient (Extended Data Table 2).

The risk ratio[24] represents the ratio between the probability of an event under the factual scenario (it is what we experienced and it is based on the observed urban intensity and rainfall) and the counterfactual scenario (it is what we would have experienced without urbanization).

Code availability. The codes related to the statistical modelling are available in Supplementary Information. The Advanced Research WRF (ARW) core of the WRF model version 3.8 was used to perform the simulations.

Data availability

The data related to the statistical modelling are available in Supplementary Information. The additional data that support the findings of this study are available from the corresponding author upon reasonable request.

31. Jin, S. et al. A comprehensive change detection method for updating the National Land Cover Database to circa 2011. *Remote Sens. Environ.* **132**, 159–175 (2013).
32. Homer, C. et al. Completion of the 2011 National Land Cover Database for the conterminous United States—representing a decade of land cover change information. *Photogramm. Eng. Remote Sens.* **81**, 345–354 (2015).
33. Chen, F. et al. The integrated WRF/urban modelling system: development, evaluation, and applications to urban environmental problems. *Int. J. Climatol.* **31**, 273–288 (2011).
34. Li, D., Bou-Zeid, E., Baeck, M. L., Jessup, S. & Smith, J. A. Modeling land surface processes and heavy rainfall in urban environments: sensitivity to urban surface representations. *J. Hydrometeorol.* **14**, 1098–1118 (2013).
35. Lee, S.-H. et al. Evaluation of urban surface parameterizations in the WRF model using measurements during the Texas Air Quality Study 2006 field campaign. *Atmos. Chem. Phys.* **11**, 2127–2143 (2011).
36. Chen, F., Miao, S., Tewari, M., Bao, J. W. & Kusaka, H. A numerical study of interactions between surface forcing and sea breeze circulations and their effects on stagnation in the greater Houston area. *J. Geophys. Res.* **116**, D12105 (2011).
37. Kusaka, H., Nawata, K., Suzuki-Parker, A., Takane, Y. & Furuhashi, N. Mechanism of precipitation increase with urbanization in Tokyo as revealed by ensemble climate simulations. *J. Appl. Meteorol. Climatol.* **53**, 824–839 (2014).
38. Holst, C. C., Tam, C.-Y. & Chan, J. C. L. Sensitivity of urban rainfall to anthropogenic heat flux: a numerical experiment. *Geophys. Res. Lett.* **43**, 2240–2248 (2016).
39. Zhong, S. et al. Urbanization-induced urban heat island and aerosol effects on climate extremes in the Yangtze River Delta region of China. *Atmos. Chem. Phys.* **17**, 5439–5457 (2017).
40. Paul, S. et al. Increased spatial variability and intensification of extreme monsoon rainfall due to urbanization. *Sci. Rep.* **8**, 3918 (2018).
41. Mesinger, F. et al. North American regional reanalysis. *Bull. Am. Meteorol. Soc.* **87**, 343–360 (2006).
42. Prosdocimi, I., Kjeldsen, T. & Miller, J. Detection and attribution of urbanization effect on flood extremes using nonstationary flood-frequency models. *Wat. Resour. Res.* **51**, 4244–4262 (2015).
43. DeWalle, D. R., Swistock, B. R., Johnson, T. E. & McGuire, K. J. Potential effects of climate change and urbanization on mean annual streamflow in the United States. *Wat. Resour. Res.* **36**, 2655–2664 (2000).
44. Gluck, W. R. & McCuen, R. H. Estimating land use characteristics for hydrologic models. *Wat. Resour. Res.* **11**, 177–179 (1975).
45. Stankowski, S. J. Population density as an indirect indicator of urban and suburban land-surface modifications. *US Geol. Surv. Prof. Pap.* **800**, 219–224 (1972).
46. Villarini, G., Serinaldi, F., Smith, J. A. & Krajewski, W. F. On the stationarity of annual flood peaks in the continental United States during the 20th century. *Wat. Resour. Res.* **45**, W08417 (2009).
47. López, J. & Francés, F. Non-stationary flood frequency analysis in continental Spanish rivers, using climate and reservoir indices as external covariates. *Hydrol. Earth Syst. Sci.* **17**, 3189–3203 (2013).
48. Slater, L. J. & Villarini, G. Evaluating the drivers of seasonal streamflow in the US Midwest. *Water* **9**, 695 (2017).
49. van Buuren, S. & Fredriks, M. Worm plot: a simple diagnostic device for modelling growth reference curves. *Stat. Med.* **20**, 1259–1277 (2001).

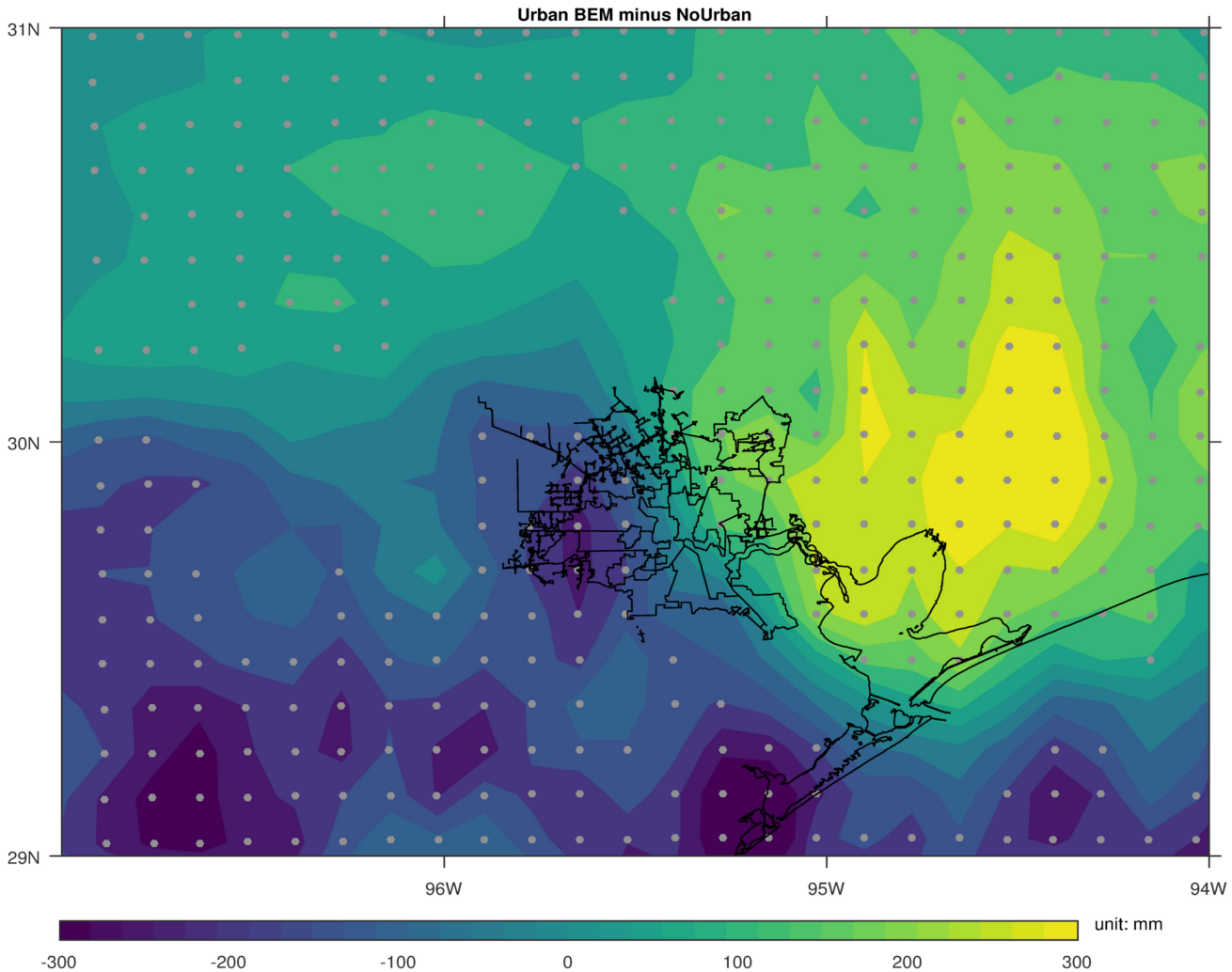

Extended Data Fig. 1 | Effect of urbanization on the storm total rainfall during hurricane Harvey. The map (the black outlines mark urban areas of Houston) shows the difference (Urban BEM minus NoUrban) in accumulated precipitation for 25 August 0 h to 30 August 0 h 2017 between the 'Urban BEM' and 'NoUrban' WRF experiments. The stippled regions represent areas for which these differences are statistically different from zero (that is, there are no effects of urbanization in terms of rainfall) at the $P = 0.05$ significance level based on Student's t test.

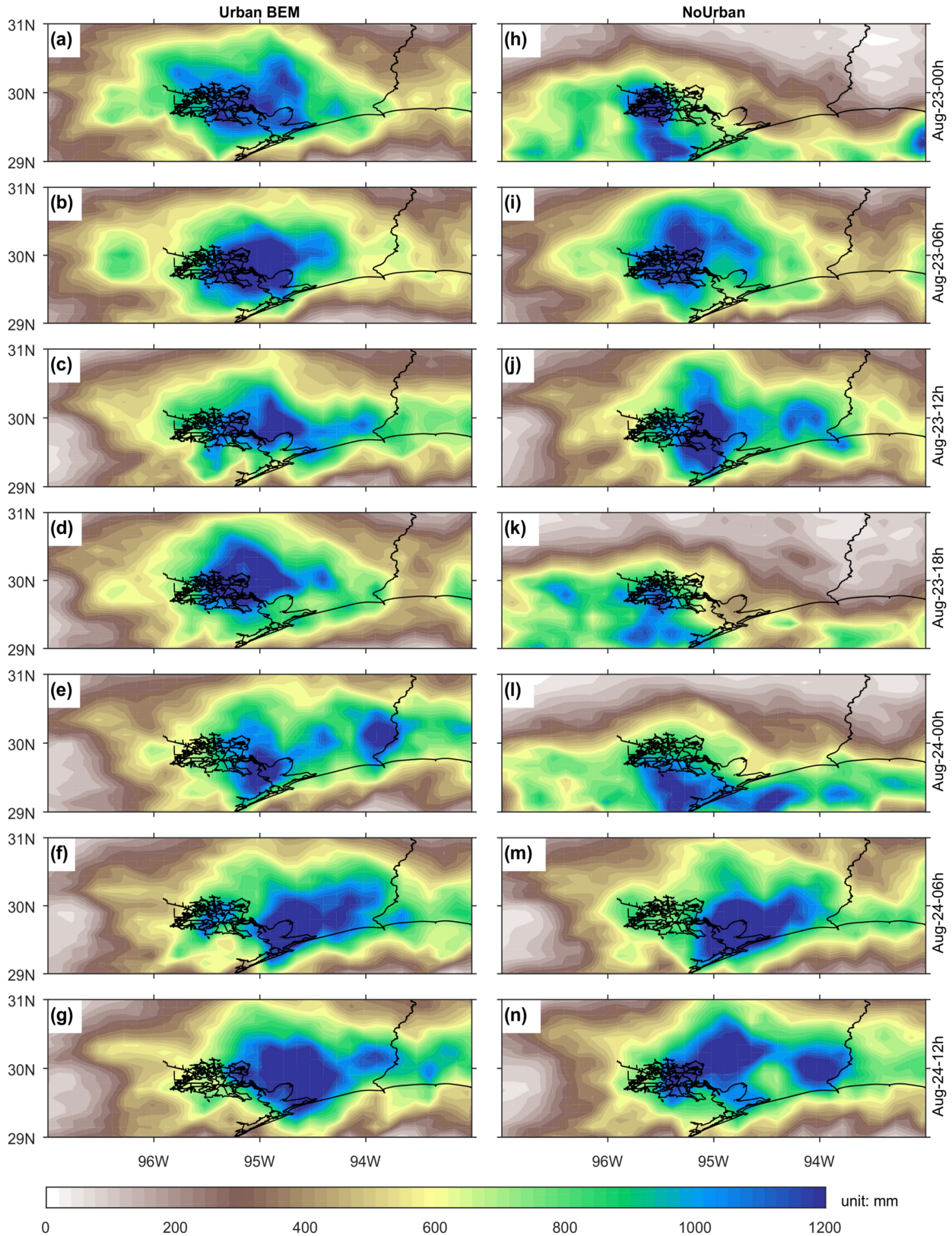

Extended Data Fig. 2 | Accumulated precipitation in each ensemble member of the WRF experiments. a–n, Accumulated precipitation (colour scale) for 25 August 0 h to 30 August 0 h 2017 in each member of the 'Urban BEM' (**a**–**g**) and 'NoUrban' (**h**–**n**) WRF experiments initialized between 23 August 0 h and 24 August 12 h at 6-h intervals.

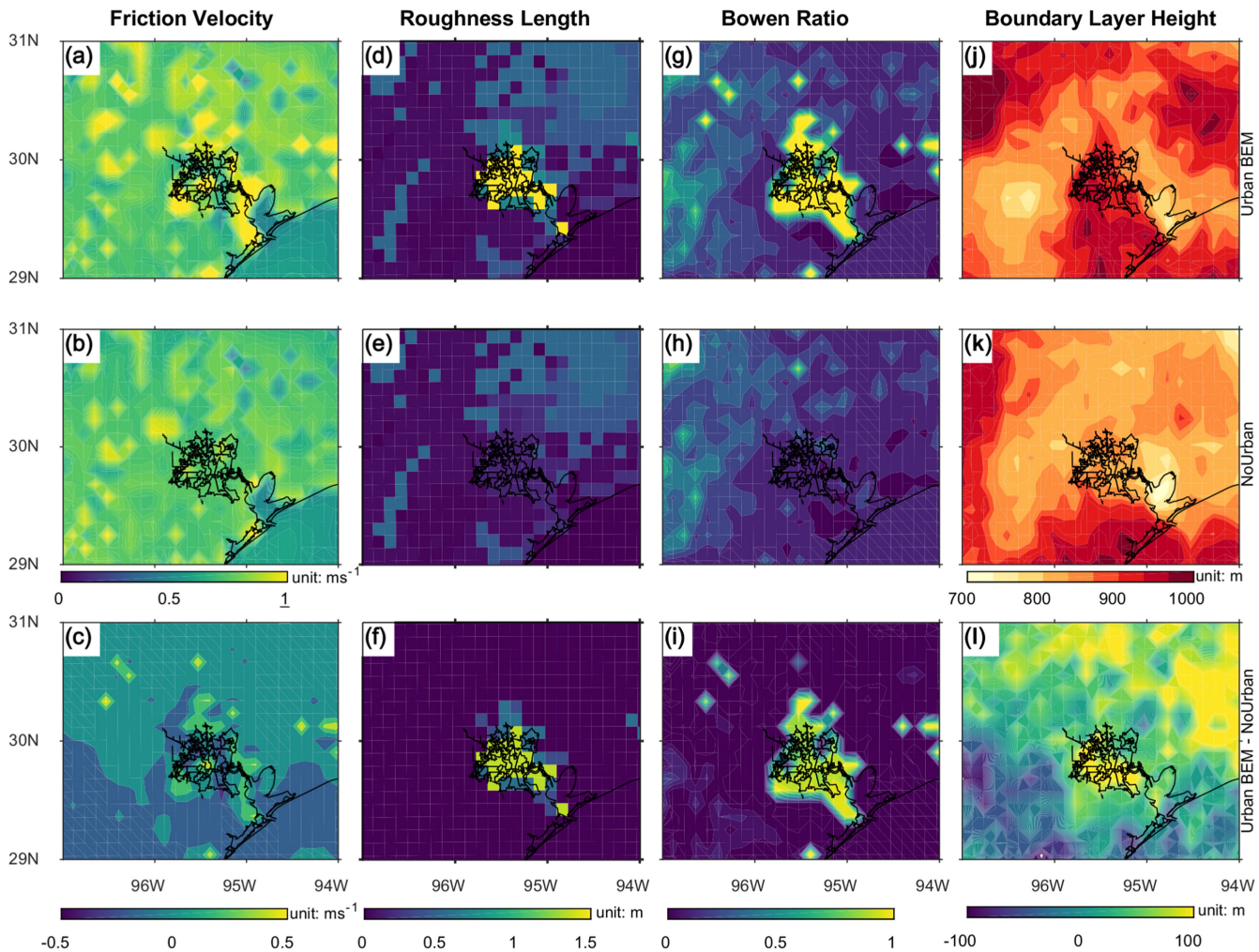

Extended Data Fig. 3 | Key variables for diagnosing the impacts of urbanization on hurricane Harvey. a–l, Friction velocity (**a–c**), roughness length (**d–f**), Bowen ratio (**g–i**) and boundary layer height (**j–l**) are shown for the 'Urban BEM' (top panels) and 'NoUrban' (middle panels) experiments with WRF and their differences (bottom panels).

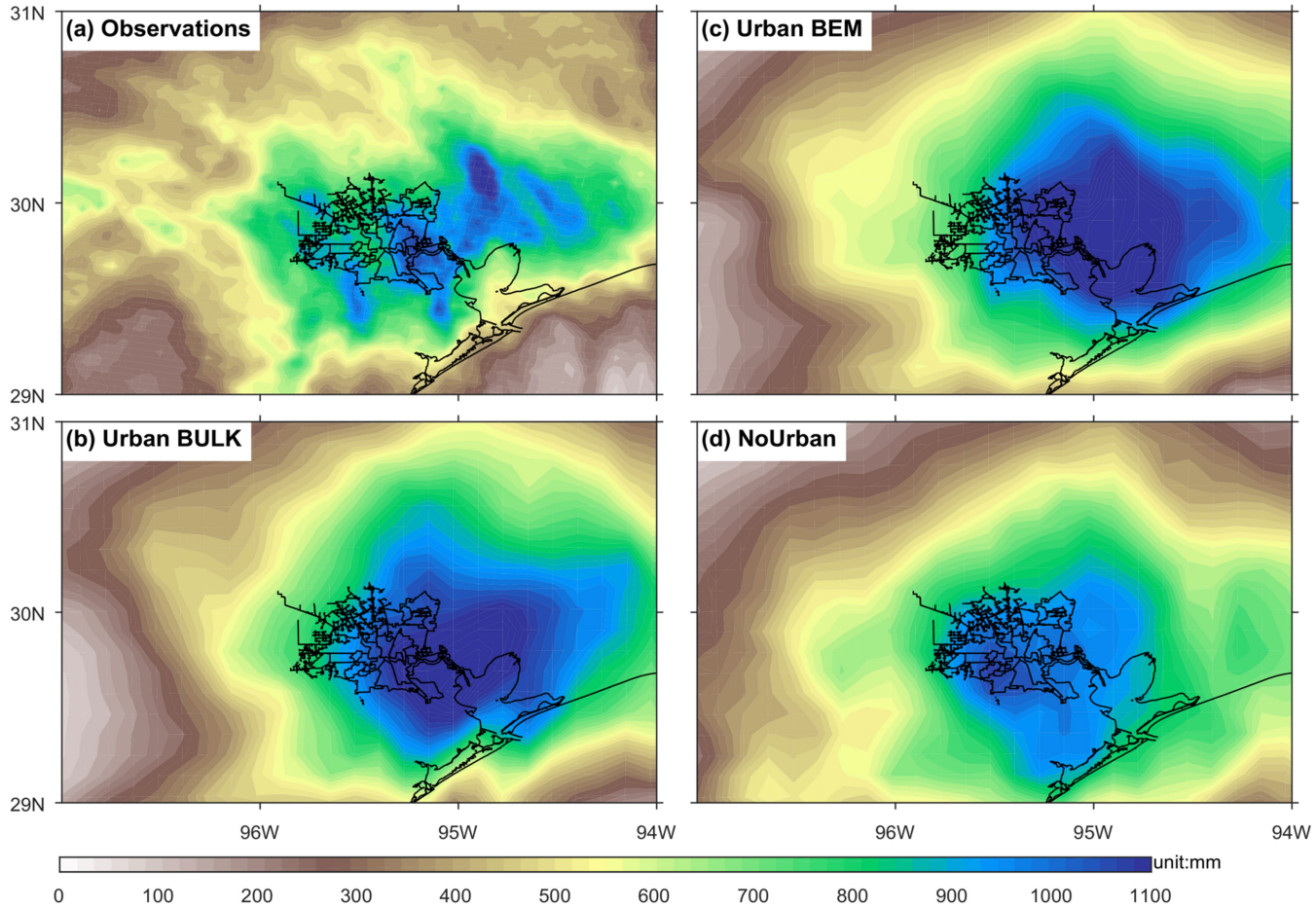

Extended Data Fig. 4 | Accumulated precipitation for hurricane Harvey in observations and different urbanization schemes and settings of WRF experiments. a–d, Accumulated precipitation (colour scale) is shown for 25 August 0 h to 30 August 0 h 2017 in observations (**a**), and in the 'Urban BULK' (**b**), 'Urban BEM' (**c**) and 'NoUrban' (in which urban land-use types are replaced by croplands; **d**) WRF experiments.

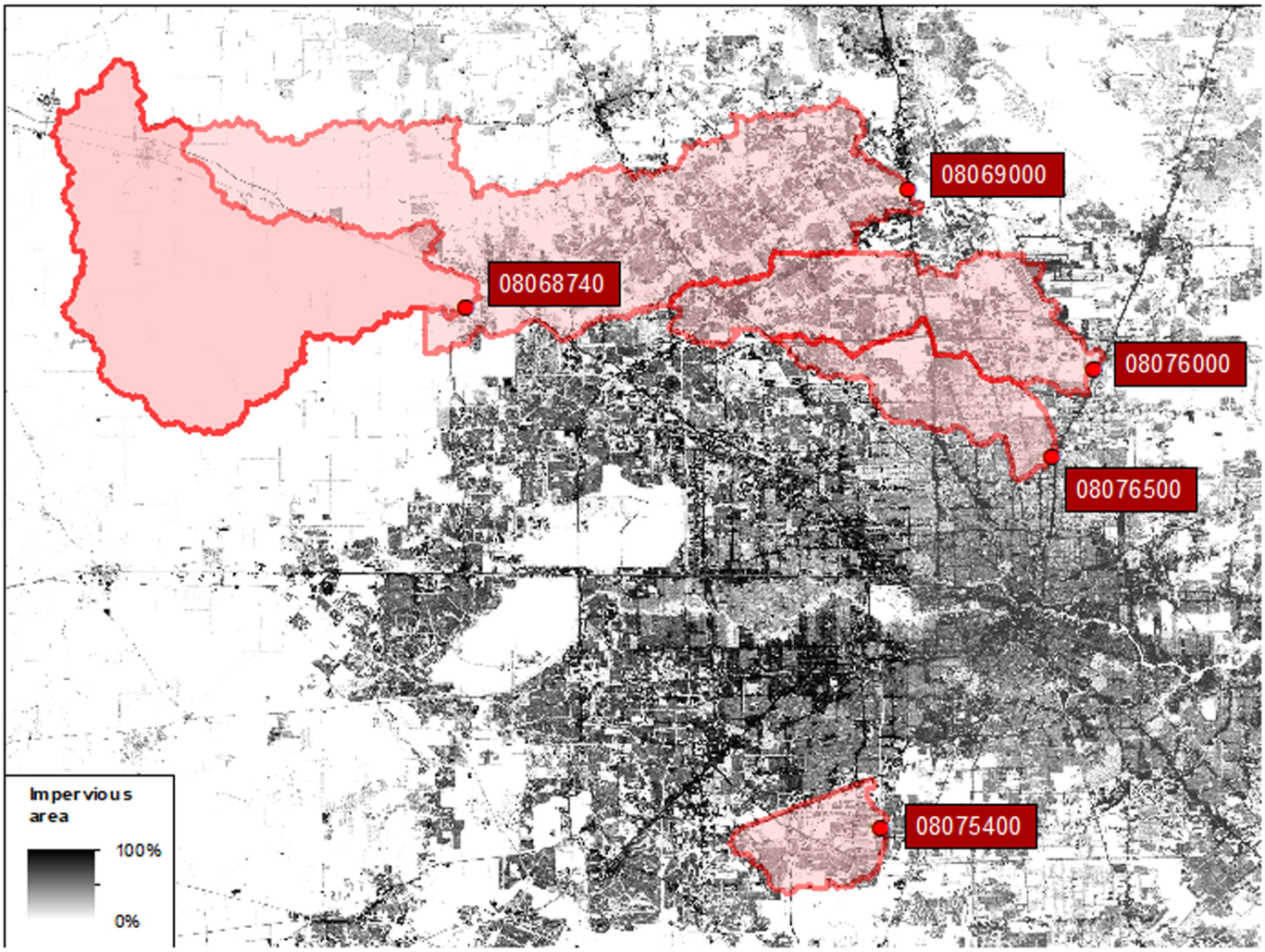

Extended Data Fig. 5 | Basin boundaries of the five watersheds considered in this study. The ID number for each basin is also shown. The percentage of impervious area is indicated by the grey scale.

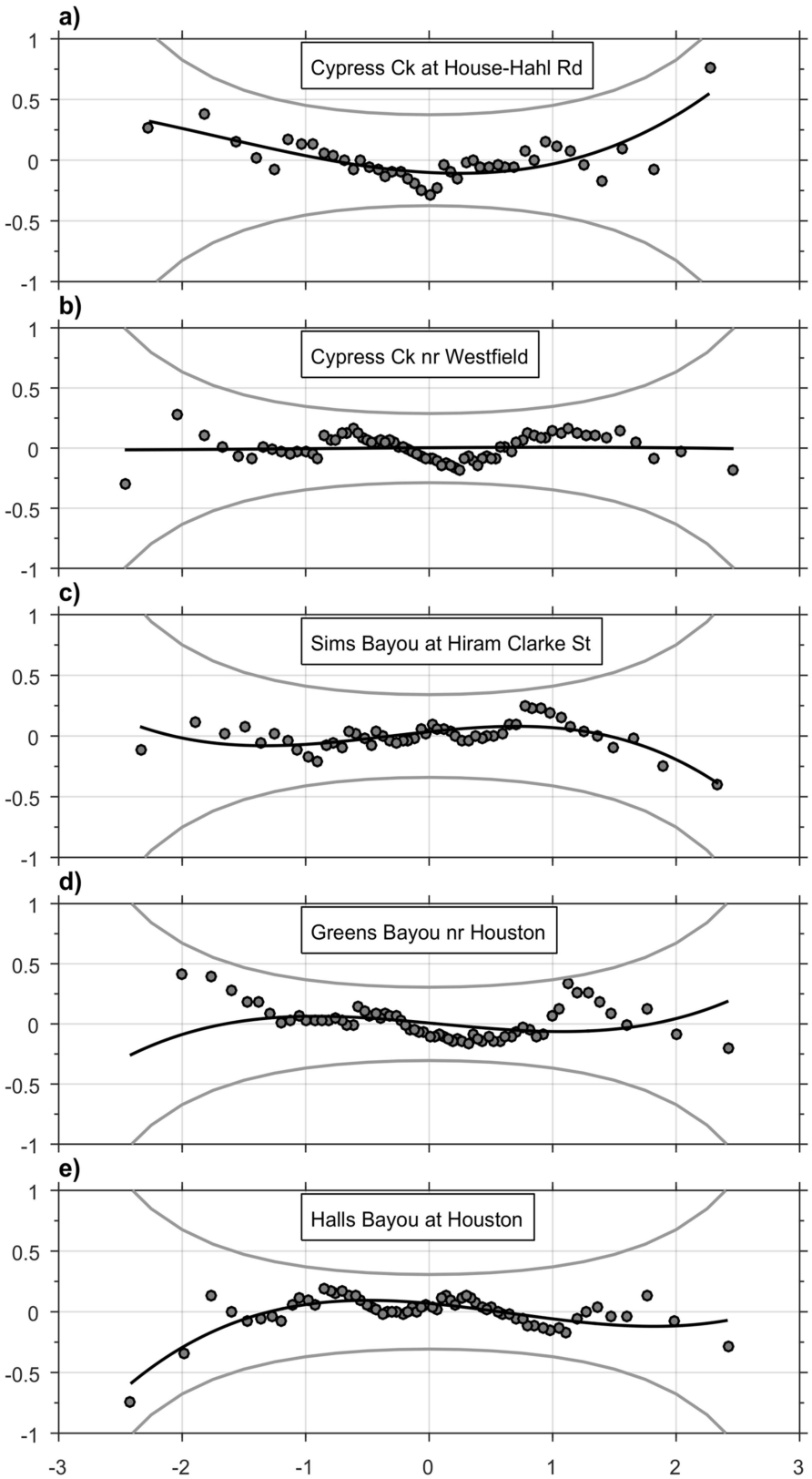

Extended Data Fig. 6 | Worm plots for the fitted models of annual maximum peak discharge records. a–e, Worm plots for the fitted models shown to evaluate the goodness of fit as shown in Fig. 3. For a satisfactory fit, the data points should be within the two grey lines (95% confidence interval).

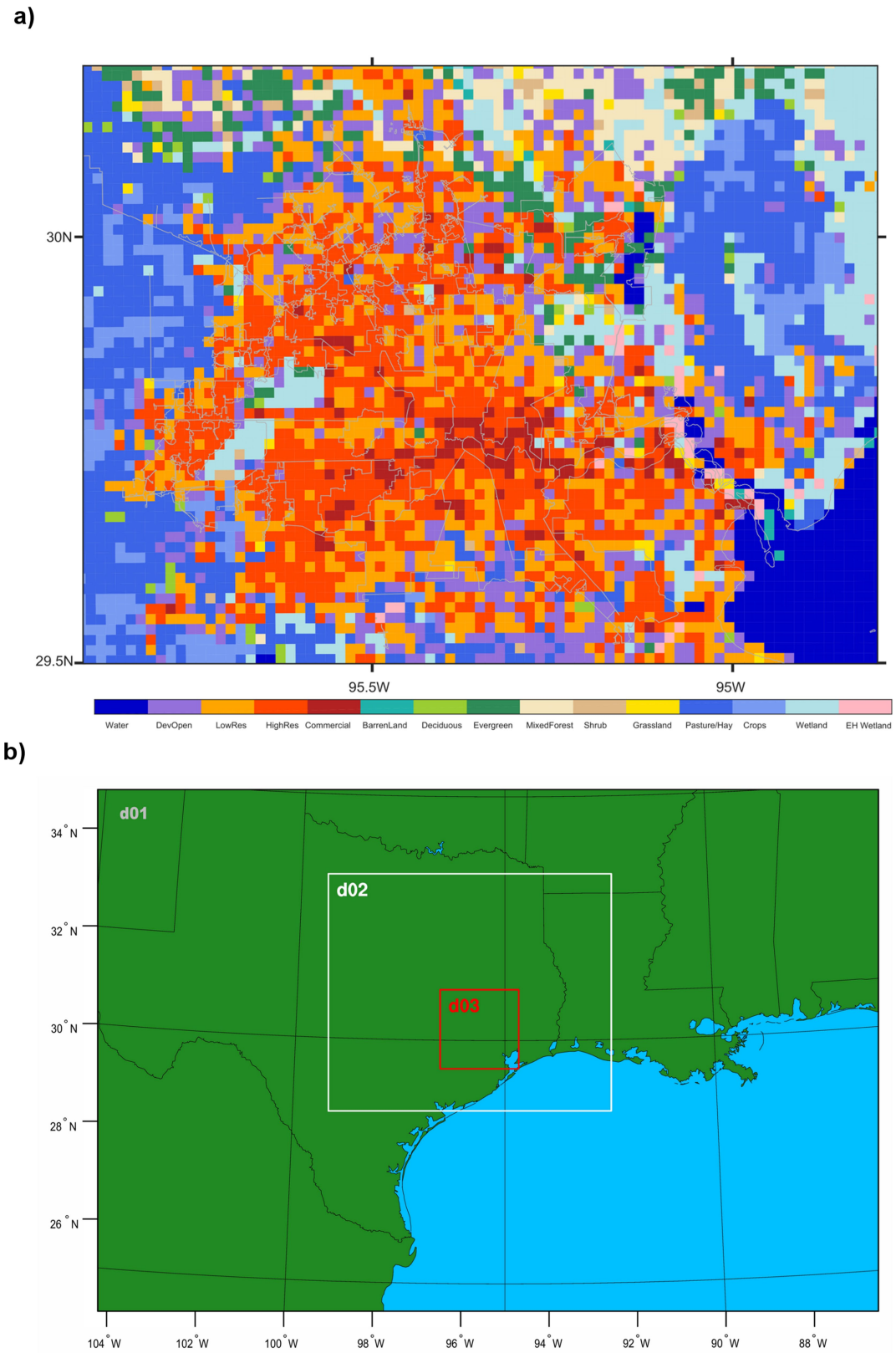

Extended Data Fig. 7 | Information related to the WRF simulations. **a**, Land-use map in the Houston area. The low-residential, high-residential and commercial land-use categories are coloured in orange, red and dark red, respectively. (DevOpen, developed open space; EH Wetland, emergent herbaceous wetlands.) **b**, Three spatial domains d01, d02 and d03 in the WRF simulations with spatial resolution of 12 km, 4 km and 1.33 km, respectively.

Extended Data Table 1 | Summary of the characteristics of the five watersheds studied and of the WRF physics options

a)

USGS ID	Name	Drainage area (mi^2)	Risk Ratio
08068740	Cypress Creek at House-Hahl Road near Cypress, TX	131	1.1
08069000	Cypress Creek near Westfield, TX	285	1.9
08075400	Sims Bayou at Hiram Clarke Street, Houston, TX	20.2	8.3
08076000	Greens Bayou near Houston, TX	68.7	91.9
08076500	Halls Bayou at Houston, TX	28.7	2.9

b)

Physics	Options
Microphysics	WSM 6-class graupel scheme
Surface layer	Monin-Obukhov scheme
Land surface	unified Noah land-surface model
Boundary layer scheme	Mellor-Yamada-Janjic TKE scheme
Cumulus parameterization	None for d02 and d03, and the Betts-Miller-Janjic scheme for d01
Longwave radiation	Rapid Radiative Transfer Model
Shortwave radiation	Dudhia scheme
Land use	NLCD2011 (40 categories)

a, Summary information about the five basins considered in this study, and the related value of the risk ratio (see Methods). **b**, Setting of WRF physics options. (WSM, the WRF Single-moment Microphysics scheme.)

Extended Data Table 2 | Summary of the modelling results for the five basins considered in this study

	08068740	08069000	08075400	08076000	08076500
Distribution	Lognormal	Gamma	Gamma	Lognormal	Gamma
Intercept (μ)	6.96 (0.12)	7.42 (0.21)	7.04 (0.35)	7.08 (0.20)	7.21 (0.17)
Rainfall (μ)	0.0068 (0.001)	0.0026 (0.0004)	0.0032 (0.001)	0.0044 (0.001)	0.003 (0.001)
Population (μ)	-	0.0051 (0.001)	0.0055 (0.002)	0.0070 (0.001)	0.003 (0.001)
Intercept (σ)	-0.51 (0.11)	-0.11 (0.20)	-0.65 (0.09)	-0.75 (0.09)	-0.94 (0.08)
Rainfall (σ)	-	-	-	-	-
Population (σ)	-	-0.004 (0.001)	-	-	-
Mean (residuals)	0.00	0.00	0.00	0.00	0.00
Variance (residuals)	1.02	1.02	1.02	1.02	1.02
Skewness (residuals)	0.55	-0.02	-0.14	-0.17	-0.41
Kurtosis (residuals)	3.27	2.77	2.29	3.83	3.51
Filliben (residuals)	0.984	0.995	0.993	0.982	0.990

The first value is the point estimate, and the value in parentheses is the standard error. The '-' symbol means that the parameter does not depend on the predictor. For the lognormal distribution the link function for the μ parameter is the identity, whereas for the σ parameter the link function is logarithmic. For the gamma distribution both parameters have a logarithmic link function.